REVISTA MATÉRIA V.31
ISSN 1517-7076 articles e20250822, 2026

Effect of treated incinerated bottom ash on the concrete properties – investigation on the long-term mechanical properties

Nirmal Kumar Krishnaswami[1], Manoj Prabhu Chinnusamy[2], Sivakumar Annamalai[3], Pradeep Thirumoorthy[4]

[1]PGP College of Engineering and Technology, Department of Civil Engineering. Keerambur, Namakkal, Tamil Nadu, India.
[2]Velalar College of Engineering and Technology, Department of Civil Engineering. Thindal, Erode, Tamil Nadu, India.
[3]Excel Engineering College, Department of Mechanical Engineering. Namakkal, Tamil Nadu, India.
[4]Kongu Engineering College, Department of Civil Engineering. Perundurai, Erode, Tamil Nadu, India.
e-mail: vppgpcet@gmail.com, manojnkcm95@gmail.com, askmechkongu@gmail.com, civil.pradeep@gmail.com

ABSTRACT

The practice of disposing of incinerated bottom ash (IBA) in landfills impose serious risk over the environment. Perhaps, the lack of fine aggregates in the building sector emphasize the use of appropriate substitutes made from industrial wastes. The potential use of treated IBA as a fine aggregate alternative in concrete is examined in this study. By varying the IBA replacement ratios and at constant w/c ratio, the impact of IBA was examined. The concrete mixes were made at 0.45 w/c ratio, and the fine aggregate was replaced with 0% to 100% IBA at 30% intervals. The physical and chemical tests of the IBA verified the presence of heavy metals and found that the concentrations were within acceptable constraints. The workability of the concrete mixes containing IBA was assessed, and the concrete properties were measured using water absorption at 7, 28, 56, and 90 days as well as compressive, flexural, and elastic modulus strength at 7, 14, 28, and 56 days. The findings show that substitution of higher proportions of IBA have an impact on workability and show decreased strength with increased water absorption properties. On the other hand, concrete characteristics at all replacement levels tend to improve with increased curing. The TGA investigation reveals the incidence of fewer $Ca(OH)_2$ peaks due to the incomplete dilution of cement matrix, whereas SEM microstructural studies show dense structure with fine aggregates and porous structure with IBA.

Keywords: Incinerated bottom ash; Curing; Strength; Water absorption; Microstructure.

1. INTRODUCTION

The urbanization and trend towards rapid rise in the population augments the generation of municipal solid wastes (MSW) globally. The generation of MSW globally has improved drastically and will tend to augment further. For instance, "***What a Waste 2.0***" from World Bank estimated 2.01 billion tons of MSW in 2016 with a prediction of 3.40 billion tons in 2050 with a 60% upsurge in the generation, wherein 1/3rd shall be mismanaged either through open burning or dumping [1]. The headline of the World bank in 2016 implies steady growth in the mid 2020 with 2.30 to 2.50 billion tons and predicted to augment by 2.60 billion tons in 2030, emphasizing the necessity for effective recycling from 2025 and beyond. The statistics on generation of MSW globally show diversified levels and approaches implemented. The USA have generated 292 million of MSW in 2018 showing a 32% recycling rate [2]. The EPA policy of USA highlights waste management through reduction at source, recycling, energy recovery etc. with prolonged management of materials. The UK reports waste recycling at a rate of 44% in 2022, showing improvement of 45% in 2023, supported through prolonged and consistent collection along kerbside. Similarly, Wales, Scotland and Northern Ireland show 55%, 42.1% and 50.2% recycling rate [3]. The Japan shows 1.7% decrease in the MSW generation in 2023 with 890 g per capita, and 5.9% reduction in landfill waste, with 19.9% recycling rate and a total of 2.0% decrease in the quantity of wastes recycled [4]. Similarly, China surpasses 40×10^8 tons in 2022, upon which only 23% were utilized effectively, rest were being dumped in the landfills [5]. However, China expanded the collection and treatment methodology reporting 215 million tones collection in 2017 to reach a recycling target rate of 35%. The India generates 60 million tons of MSW annually with 95% collection rate of which only 50% were recycled and the

Corresponding Author: Manoj Prabhu Chinnusamy Received on 27/09/2025 Accepted on 14/01/2026

DOI: https://doi.org/10.1590/1517-7076-RMAT-2025-0822

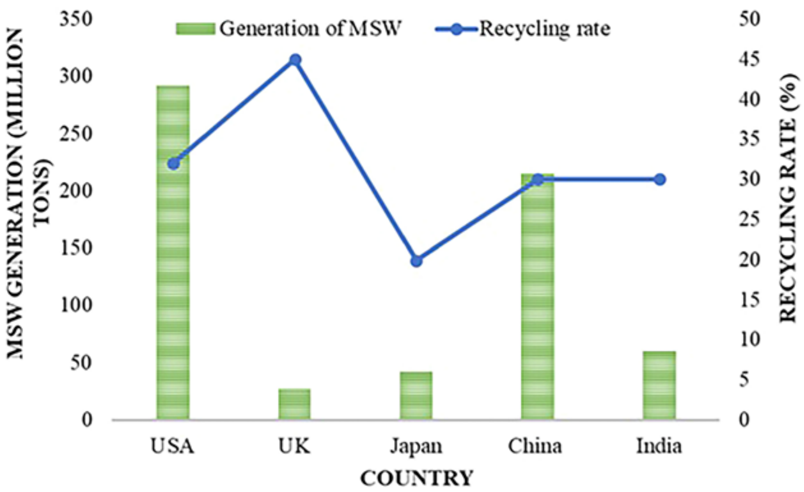

Figure 1: MSW generation and recycling rate.

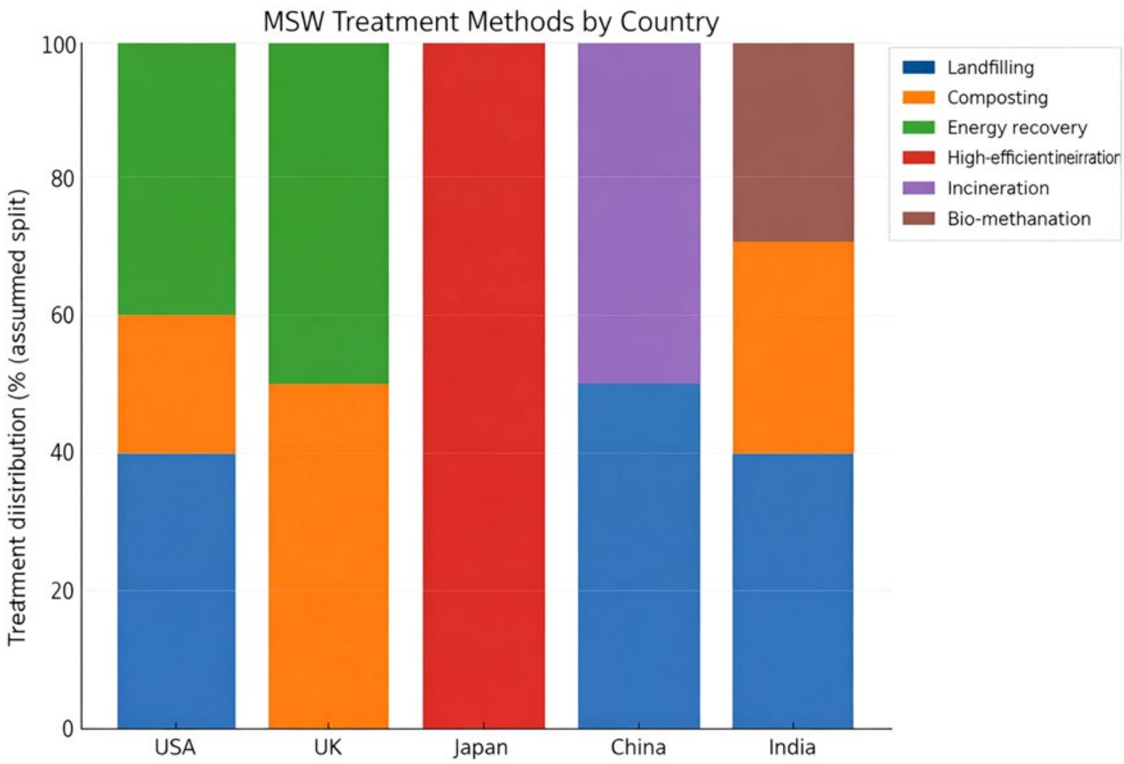

Figure 2: MSW treatment methods.

rest were being dumped. The 2016 MSW rules mandated door step collection, segregation and processing of the collected wastes [6]. Figure 1 shows the generation rate and recycling rate of MSW in various countries. Figure 2 shows the stacked representation of MSW treatment methods adopted by various countries.

Despite substantial improvement in the management of MSW around the globe, the safe disposal of MSW remains challenging. Landfilling, being the traditional practice of MSW disposal, it seems unrecognized owing to excess utilization of land resources, leachate generation, landfill gas emission etc. [7]. In USA and India, 50% of MSW were dumped in landfills leading to contamination of groundwater and degradation of land [2, 6]. The next processing technology incineration being widely adopted by developed countries like Japan, EU etc. possess constrains owing to high operation costs and concerns towards atmospheric pollution [8]. This necessitates the exploration on effective utilization of incinerated bottom as (IBA) from MSW as a value-added product. The IBA from MSW was used as SCM [9, 10], aggregates in asphalt pavement [11, 12], and as aggregates in the concrete [13, 14]. The IBA was also used in the production of blocks and bricks [15, 16] and as filler material in the construction and roads [17]. Among all, utilization as aggregates in the concrete was effective owing to the less energy-intensive processing method, scarcity of natural aggregates and sustainability concerns.

Several researches have been conducted with the use of IBA as SCM, aggregates etc. in the concrete. Sun *et al.* [18] investigated the use of IBA as aggregate in asphalt mixture and observed that 6% substitution in concrete improved strength by 10.7% and 20% substitution in asphalt mixture improved the resistance to moisture and tensile strength. Life-cycle analysis shown 22% higher footprint but 2100 tons of aggregate was saved. Complementarily, Olea *et al.* [19] assessed the reuse potential of IBA in UK as aggregates through mineralogical and chemical analyses and observed that IBA show higher pH (11%) and higher traces of metals like Cu, Zn at pH < 6. The study suggested that higher percentages of Si, higher pH and lesser POP of IBA makes its suitable as construction material in low-environmental risk areas. Fan *et al.* [20] used IBA as fine aggregates and fly ash and GGBS as SCM to produce ecofriendly concrete. It was observed that utilization of fly ash with GGBS in IBA incorporated concrete show lower strength. However, the use of either fly ash or GGBS with IBA show improved strength after 7 days. It was also observed that substitution of environmentally friendly mortar lowers the leaching effect of IBA in the concrete. The life cycle analysis reveals 5% reduction in the energy consumption, 12% reduction in CO_2 emission and 63% reduction in the cost with IBA for 1 m^3 of concrete. Yao *et al.* [21] substituted IBA as fine aggregate and observed that strength was improved up to 42% at 3 days, but lowered by 13% at 150 days compared to CC. The higher absorption characteristics of IBA lowers the workability of the mixes. The substitution of IBA improves the early age strength but lowers the long-term strength. The leachate analysis signifies the acceptable limits on the toxicity level of metals in the IBA used.

Conversely, Huynh and Ngo [22] observed reduction in the strength with higher percentages of IBA. The workability and density reduce with higher percentages of IBA owing to the absorptive nature and lower density of IBA lowers the workability and density of concrete. The complete substitution of IBA lowers the strength by 48%. Similarly, other durability properties such as shrinkage, chloride ingression and sulphate ingression increase with increase in the substitution of IBA. Alderete *et al.* [23] used processed IBA as substitute to cement and observed optimal replacement as 20%. Three different cement CEM I 52.5 N, CEM II B-V 32.5 R and CEM I 52.5 R were used along with processed IBA and it was observed that use of 20% of IBA with blended cement performs better. Liu *et al.* [24] used FA and silica fume as SCM with OPC and IBA as fine aggregate and found that use of 50% of 50% well-graded IBA show improved strength. The strength ranges from 15 to 22 MPa at 28 days satisfying the requirements for structural repairs. The water absorption ranges from 8 to 10% owing to the absorptive nature of IBA. The leachate analysis indicate that heavy elements are within the acceptable limits signifying its utilization as fine aggregate. Joseph *et al.* [25] pretreated IBA by immersing in water at 105 ^oC for 24 hours and observed that optimal substitution of 25% show 85% of control mortar strength at 90 days. The average increase was observed to be around 50% with treated IBA compared to untreated and nearly 75% control concrete strength was achieved with treated IBA. Ren *et al.* [26] developed artificial aggregate with IBA and incinerated fly ash through pelletization technique. The use of 40% artificial aggregate shows a bulk density in the range of 890 to 1075 kg/m^3 with 5.7 MPa strength. The use of incinerated fly ash lowers the heat with formation of lesser hydration compounds. However, with GGBS and incinerated fly ash, ettringite formation improves the aggregate strength. The concrete with artificial aggregate show strength more than 45 MPa. Such attribute is due to the internal curing and pozzolanic reactivity of artificial aggregates in ITZ.

Several researchers have used IBA in special concrete applications. For instance, Chimenos *et al.* [27] investigated the feasibility of using IBA as precursor in Geopolymer mortar and observed up to 35 MPa strength at 28 days making it suitable for paving applications. The incidence of C-A-S-H and N-A-S-H improves the strength and balances the chemical stability. Similarly, Wang *et al.* [28] developed alkali-activated slag concrete with various proportions of IBA and found the optimal substitution as 50% with a strength of 43 MPa. The leaching rate was observed to be low with strength loss up to 1.7% upon exposure to sulphates. The synergistic effect of IBA with sand results in compact microstructure and thus ensues in better concrete properties. Furthermore, Wang *et al.* [29] used IBA in high-performance concrete and found strength and elastic modulus was lowered upto 17% and 13% respectively. The shrinkage and chloride ingression was also increased by 13% and 24% than CC. The higher pore volume with the substitution of IBA attributes to the inferior concrete properties, however the CO2 emission and cost lowers. The research towards valorization of IBA have increased in recent times, yet its suitability as construction materials remains inadequate owing to environmental, technical and regulatory alarms. The chemical constituents of IBA that contains heavy metals, salts results in leaching that affects durability of the concrete. Earlier research have reported that with the use of IBA as aggregates, the workability reduces owing to its higher porosity, resulting in reduced strength. However, more studies focus on partial substitution in mortar with limited discussions on its long-term behaviour. Concerning the sustainability, use of IBA as substitute to aggregate lowers mining of natural resources and supports in mitigating the ecological impacts. Furthermore, limited studies on IBA on long-term mechanical and microstructural properties needs attention. Considering the above limitations, the current research investigates the influence of treated IBA on the long-term mechanical and microstructural behaviour of concrete with treated IBA as fine aggregate at various replacement levels.

2. MATERIALS AND METHODS

2.1. Processing of IBA

Figure 3 shows the schematic illustration on the processing of IBA. The IBA obtained from the MSW incineration plants necessitates methodical processing prior to its use as fine aggregates in the concrete. Initially, the obtained IBA was visually inspected to eliminate huge boulders of non-combustible and metallic impurities. The large boulders are crumpled to breakdown the cumulations without the formation of excessive fines. The IBA was then fed through magnetic separation unit to remove Fe impurities, subsequent by screening to separate the vital IBA fractions with relative particle sizes of 2.36 mm~4.75 mm, which equivalents the fine aggregate grading. The separated fraction was washed thoroughly with potable water to decrease the dust fractions, light impurities and soluble salts and the washing was continued till the conductivity and pH of water were within the tolerable limits. The IBA fraction were then oven-dried at 105 ± 5 °C for 24-hours to attain constant weight and kept in an air-tight containers for subsequent substitution as fine aggregate. Several researches [30–33] infer that systematic treatment of IBA reduces the metal solubility and improves its reactivity, making it appropriate as sustainable construction material. Table 1 shows the chemical constituents of materials and it is observed that heavy metals of IBA are within the limits. OPC 53 grade cement [34] and potable water as per IS 456 was used in the research [36]. Table 2 shows the aggregate properties [35]. Figure 4 shows the gradation curves of aggregates.

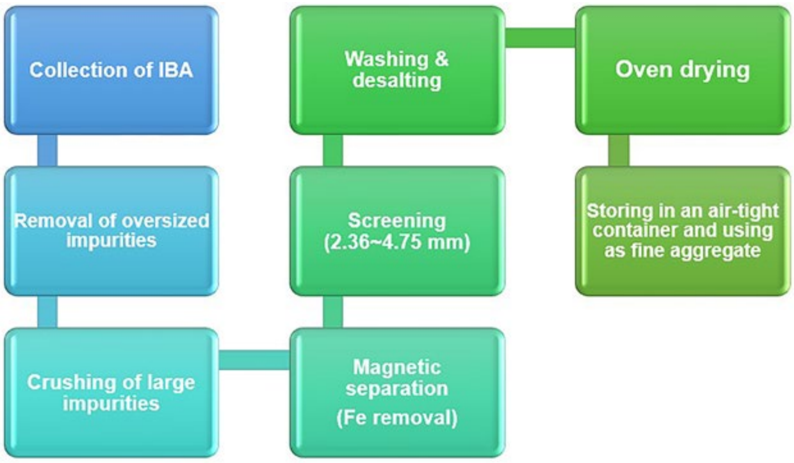

Figure 3: Processing of IBA.

Table 1: Chemical constituents of materials.

OXIDES	OPC (%)	RS (%)	RG (%)	IBA (%)
SiO_2	21.45	65.16	62.43	47.13
Al_2O_3	6.24	16.43	15.17	12.67
Fe_2O_3	3.70	7.31	6.90	8.53
CaO	63.51	4.12	5.23	20.87
MgO	2.42	2.53	3.27	3.41
SO_3	2.85	0.51	0.36	2.05
Na_2O & K_2O	1.11	1.23	1.11	3.89

Table 2: Aggregate properties.

PROPERTIES	RS	RG	IBA
Specific Gravity	2.61	2.73	2.20
Bulk density (kg/m^3)	1614	1530	1274
Water Absorption (%)	1.10	0.76	6.73
Fineness Modulus	2.74	6.73	2.54

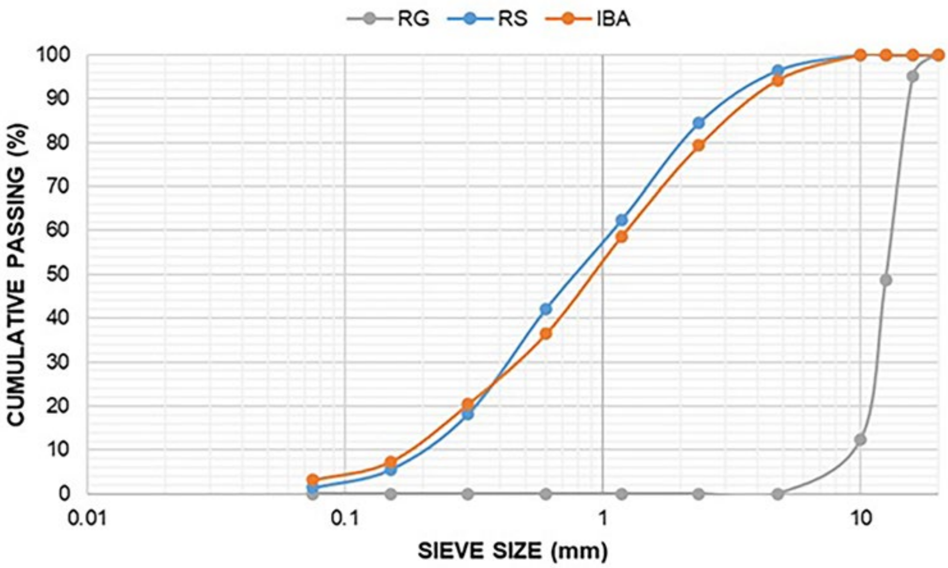

Figure 4: Gradation curves of aggregates.

Table 3: Quantities of concrete raw materials.

	(kg/m^3)				
	OPC	RS	IBA	RG	WATER
IBA0	435	610	0	1160	195
IBA30	435	427	183	1160	195
IBA60	435	244	366	1160	195
IBA90	435	61	549	1160	195
IBA100	435	0	610	1160	195

2.2. Methodology

Table 3 shows the raw materials quantities used in the concrete mix preparation [37]. The RS was replaced with IBA from 0% to 100% at intervals of 30% with mixes designed as IBA0, IBA30, IBA60, IBA90 and IBA100 prepared at 0.45 w/c. For instance, IBA30 indicated the concrete mixes are prepared with 30% IBA and 70% RS at 0.45 w/c. Though IBA absorb more water, the mixes were prepared without SP so as to investigate the intrinsic behaviour of IBA. The manufactured concrete for each designated mixes were cast into various shapes of cubes, cylinders and prisms, laboratory-dried for one day. After required time, the samples were removed from moulds and cured under laboratory conditions. The fresh property of the concrete mixes was assessed after the concrete preparation with compaction factor [38]. The mechanical properties of the IBA concrete were evaluated using 150 mm cubes [39], 500 × 100 × 100 mm prisms [40], and 150 mm × 300 mm cylinders [41] to measure the compressive-strength, flexural-strength and elastic-modulus (EM). The water-absorption of IBA concrete was evaluated with 150 mm cubes [42]. After being oven-dried at 100 ºC, cooled, and weighed as W1, the cubes were submerged in water for the required period, surface-dried, and weighed as W2. The WA of the IBA concrete was obtained as the mass difference in terms of percentage.

3. RESULTS AND DISCUSSIONS

3.1. Characterization studies on aggregates

Figure 5 the characterization parameters of RS and IBA used. Figure 5(a) shows the XRD of the IBA and RS used that emphasizes the mineralogical characteristics of RS and IBA. The XRD pattern of RS reflects strident crystalline peaks of SiO_2, attributing its stable and inert nature, that substantiates the strength through C–S–H formation and effective particle packing. However, IBA reflect crystalline peaks such as $CaCO_3$, $Al_6Si_2O_{13}$ and feldspar in addition few amorphous peaks. The incidence of $CaCO_3$ recommends carbonation upon storage, whereas $Al_6Si_2O_{13}$ incidence reflects in pozzolanic activity and the amorphous SiO_2 and Al_2O_3 can interact with $Ca(OH)_2$ to produce supplementary C–S–H, resulting in enhanced concrete properties upon utilization long-term strength and durability [43]. Figure 5(b) shows the TGA curves of RS and IBA. The TGA of RS show negligeable mass loss till 1000 °C, signifying its inert nature and thermal stability, with minimal reductions owing to moisture on its surface and impurities. However, IBA reflect substantial mass loss at various intervals: < 200 °C, show elimination of bound water; at 200–400 °C, reflect to disintegration of hydrated compounds and a maximum loss between 600–750 °C, owing to decomposition of $CaCO_3$ to CO_2 and CaO. Such decomposition emphasizes the incidence of CaO, that is advantageous for supplementary hydration [44]. Figure 5(c) shows the microstructure of RS and Figure 5(d) shows the microstructure of IBA. The microstructure of RS is

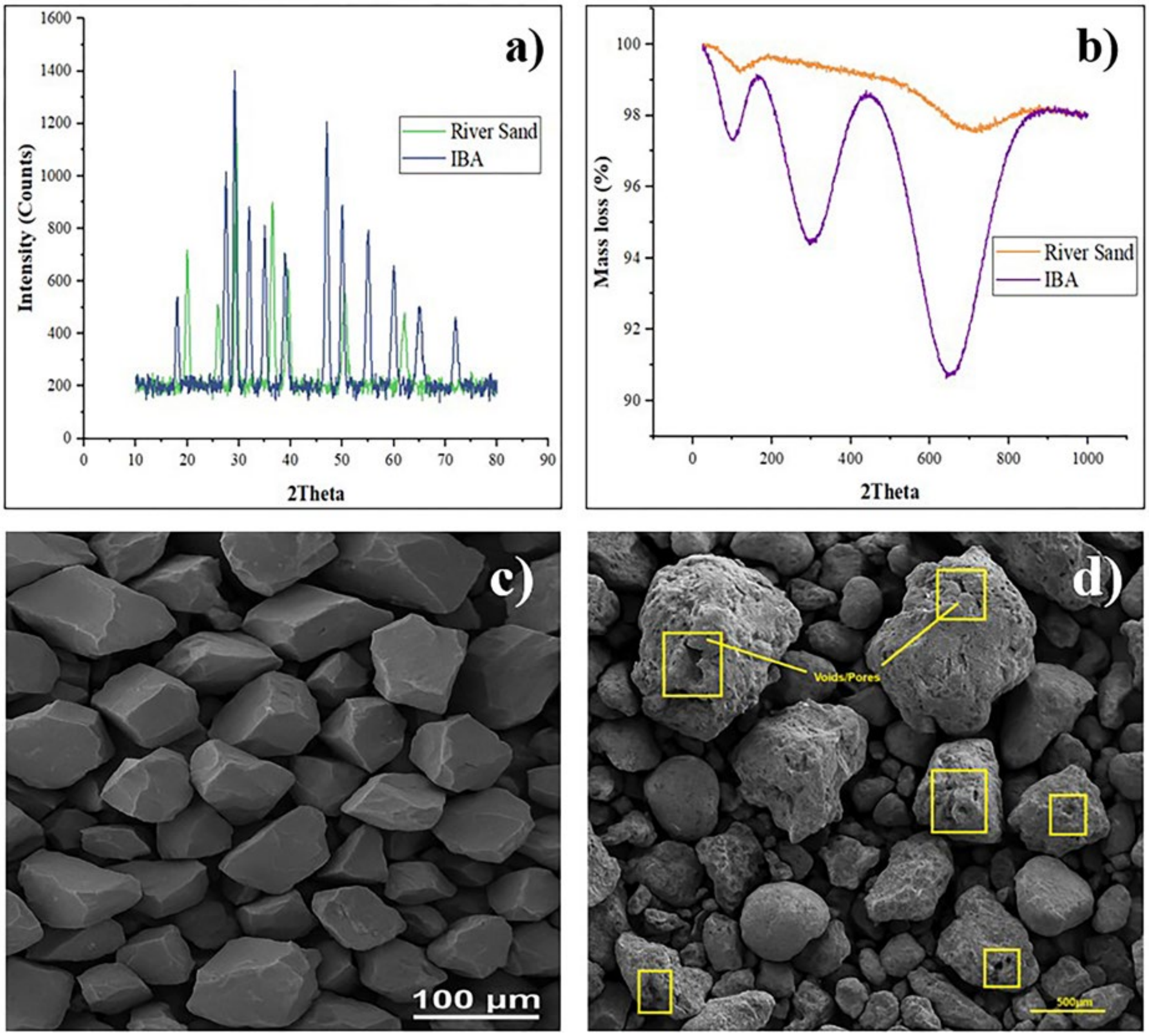

Figure 5: Characterization parameters (a) XRD, (b) TGA, (c) SEM (RS), (d) SEM (IBA).

angular with better interlocking property and smooth texture that reduces the water requirement and enhances workability. However, the microstructure of IBA show incidence of pores on/inside resulting from rapid quenching.

3.2. Workability

Figure 6 shows the compaction factor values of concrete with various percentages of IBA. The mix IBA0 reflect a compactability distinctive of well-proportioned concrete 0.45 w/c mix. However, with increase in the substitution of IBA, the compaction factor reduces gradually. The IBA particles are irregular, rough and angular, while RS is round and smooth. Such surface texture of IBA augments the interlock and internal friction, resulting in less flowable concrete and difficult to compact under normal energy, thus lessening the compaction factor [44, 45]. Furthermore, the surface texture of IBA possess pores with higher surface area that augments the water requirement, that lowers the free water availability in the mix. Such attribute lowers the entrapped air and compatibility in the concrete. The excess fines in the IBA increases the viscosity and yield stress, reducing the compaction of the concrete. Also, the unburnt carbon, carbonates and reactive compounds in the IBA absorbs water further causing water demand in the mixes and lowering the workability [46, 47].

3.3. Compressive strength

Figure 7 provides the compressive strength of the concrete mixes with IBA at various curing ages. The strength in compression for concrete mixes lowers significantly with the higher substitution of IBA. For instance, the reduction relative to IBA0 was 5.8% for IBA30, 14.43% for IBA60, 27.38% for IBA90 and 33.00% for IBA100

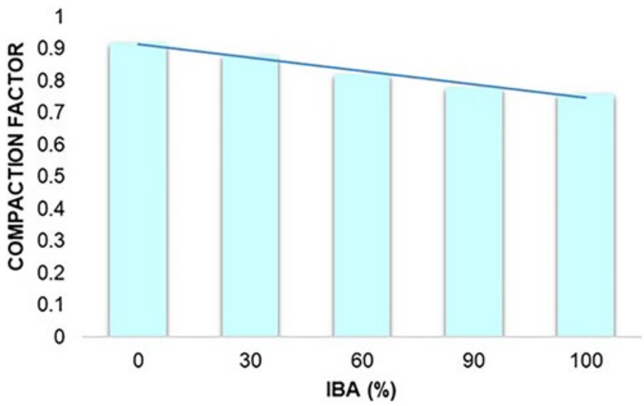

Figure 6: Compaction factor.

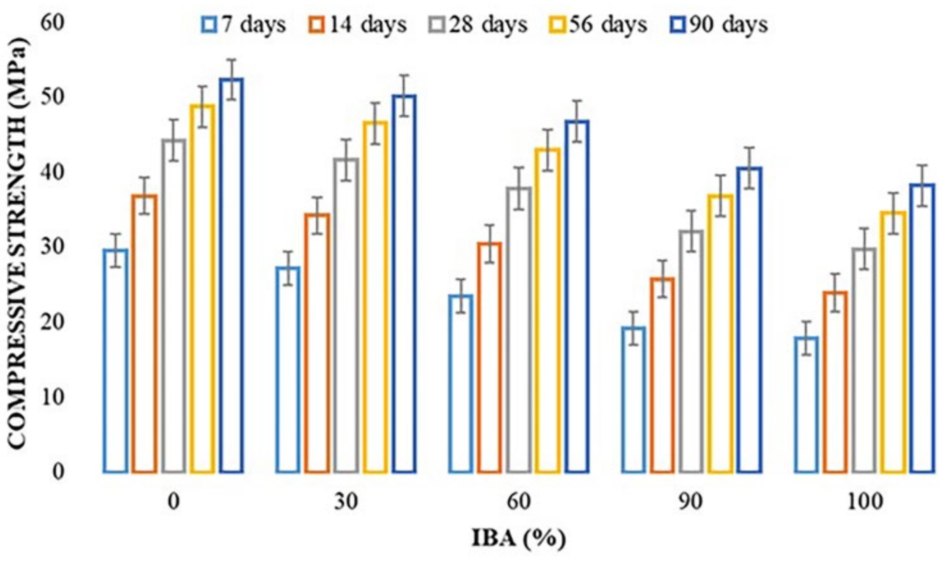

Figure 7: Compressive strength.

at 28 days. Nevertheless, the strength reduction was lower showing 4.12% for IBA30, 26.45% for IBA100 at 90 days, indicating strength recovery under prolonged curing. Significantly, the gain in the strength between 28 and 90 days was more in the mixes with IBA showing augmentation up to 29% than the control mix exhibiting 18%. Such attribute signifies the delay in the pozzolanic reactivity of IBA. The early strength reduction was attributed to (i) porous surface texture and angularity that lowers the particle packing and augments the voids in the micro-structure (ii) more water requirement owing to porous texture that reduces the free water availability required for hydration. Upon prolonged curing, the silicates and aluminates in IBA interacts with $Ca(OH)_2$ formed upon hydration to produce supplementary C–S–H that refines the microstructure. Similar observations of early strength reduction and prolonged strength enhancement was observed by [48–50], that emphasized the proper processing of IBA can enhance the pozzolanic reactivity in the concrete.

3.4. Tensile strength

Figure 8 provides the tensile strength of the concrete mixes with IBA at various curing ages. The tensile strength tracked a similar trend to compressive strength however reflected a minimum strength drop. For instance, the reduction relative to IBA0 was 4.38% for IBA30, 11.15% for IBA60, 20.43% for IBA90 and 23.27% for IBA100 at 28 days. The strength variation was influenced by both strength of the paste and the interfacial transition zone (ITZ). The porous and angular texture of IBA affects the ITZ through the formation of micro-cracks upon stress, resulting in the strength reduction [44, 45]. Nevertheless, the strength reduction was lower showing a range of 4.24% to 20.43% with prolonged strength improvement of 14 to 18% over all IBA mixes than 14.23% in the IBA0. However, supplementary C–S–H formed through the pozzolanic reactivity of IBA lids the micro-cracks around ITZ and strengthens its resulting in the long-term strength gain [51, 52]. Joseph *et al.* [53] observed strength reduction of concrete with IBA owing to inferior ITZ, yet further reported that treatment of IBA improved the particle packing and improved the strength.

3.5. Flexural strength

Figure 9 provides the flexural strength of the concrete mixes with IBA at various curing ages. The flexural strength reduced gradually with the substitution of IBA. For instance, the reduction relative to IBA0 was 5.08% for IBA30, 11.58% for IBA60, 21.34% for IBA90 and 26.62% for IBA100 at 28 days. However, at 90 days, the reduction relative to IBA0 was 4.14% for IBA30, 9.25% for IBA60, 17.79% for IBA90 and 21.24% for IBA100. Significantly, the relative enhancement from 28 days to 90 days was more in the mixes with IBA mixes than in the control mix showing only 14%. Such attribute show an equilibrium between positive pozzolanic activity of IBA and negative effects such as higher porosity and dilution [25, 26]. The flexural strength is specifically subtle to surface fissures and propagation of it that enlightens the early age failure of IBA mixes due to bending. The angular texture of IBA reflects more stress concentration and weakens the bridging ability upon cracks, ensuing in reduced strength [31, 32]. However, upon prolonged curing, formation of hydration compounds due to pozzolanic activity refines the pores and densifies the ITZ reflecting the slow propagation of cracks and thus moderate strength recovery was observed. Siddique [44] emphasized the sensitive flexural behaviour of concrete

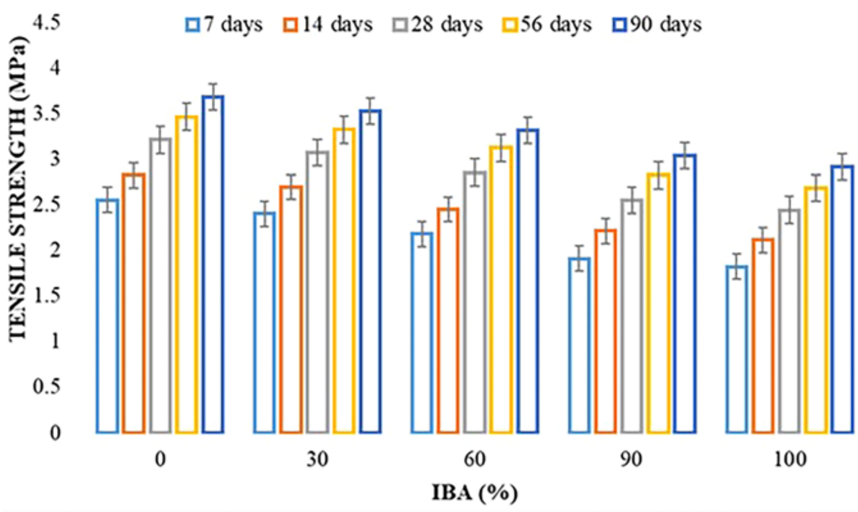

Figure 8: Tensile strength.

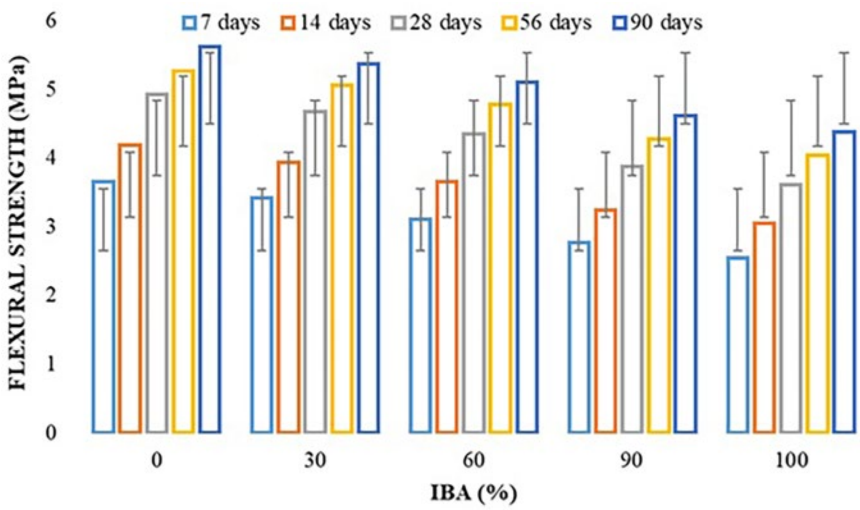

Figure 9: Flexural strength.

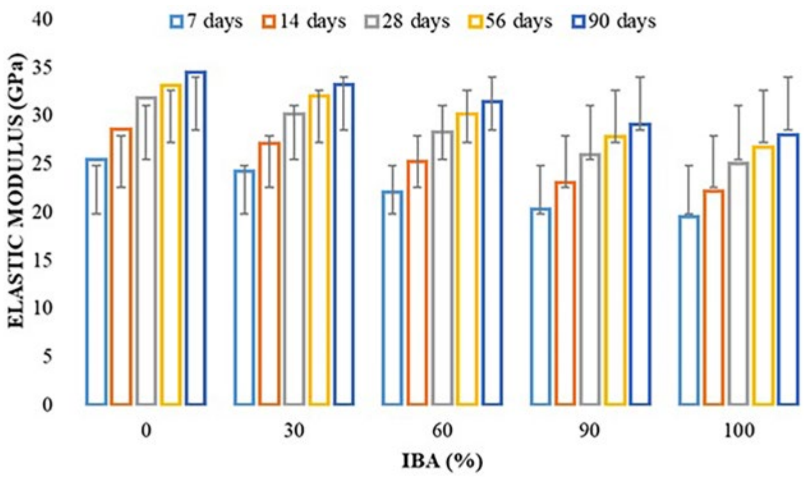

Figure 10: Elastic modulus.

with porous and angular IBA and rapid crack growth upon flexure than compression. Similarly, Zhang *et al.* [54] also observed strength reduction upto 30% at early ages, while upon prolonged curing the strength loss was minimized.

3.6. Elastic modulus

Figure 10 provides the elastic modulus of the concrete mixes with IBA at various curing ages. The elastic modulus lowered from 4.93% for IBA30 to 21.36% for IBA100% at 28 days, but curing for 90 days show reduction of only 3.76% for IBA30 and 18.43% for IBA100 mixes. Although strength regain was more distinct, recovery of elastic modulus was moderate as modulus is a direct dependent on aggregate stiffness. The reduction is the impact from the combined attribute of porous texture, angularity and weak ITZ that influence the load transfer [48, 49]. The RS possess rounded, hard and dense quartz particles with higher elastic modulus that contribute to the concrete stiffness. However, IBA was irregular with porous texture having a lower stiffness than RS. The lower stiffness of IBA ensues from the heterogenous mineralogical characteristics that contains metal oxides, unburnt carbon, Ca enriched silicates etc. [51]. The substitution of RS with IBA makes the aggregate structure less rigid, resulting in reduced load transfer.

The higher porosity of IBA augments the voids internally and these voids reflects higher stress concentration upon loading, resulting in crack formation at relatively lower stresses itself. Such characteristics of micro-crack formation lowers the slope in stress-strain curve resulting in lower elastic modulus. The ITZ was another parameter that relatively influences the elastic modulus of the concrete. The mixes with RS possess ITZ with minor micro-cracks, whereas the mixes with IBA exhibit thicker ITZ with more micro-cracks owing to the porous characteristics of IBA. This relatively weakens the adherence of IBA with matrix lowering the transfer of stress across the ITZ. Prolonged curing influences the elastic modulus of the concrete with IBA. The 7–11% improvement in the elastic modulus from 28 to 90 days are subsequent from the densification of matrix with the formed C–S–H gel. The IBA rich in Ca involves in pozzolanic interaction with $Ca(OH)_2$ formed during hydration, resulting in the formation of C–S–H [52–54].

3.7. Water absorption

Figure 11 shows the water absorption of concrete mixes with IBA at various curing ages. The water absorption increases with the higher substitution of IBA. The water absorption of IBA30, IBA60, IBA90 and IBA 100 was 5.83%, 14.48%, 24.13% and 28.18% relatively higher than IBA0. The dense, round and round porous texture of RS results in lower absorption, while the porous and angular texture of IBA results in higher absorption. The pores on/in the IBA acts as reservoirs, that captivates more water resulting higher absorption than RS. Also, the ITZ between aggregate and the matrix governs the water transport. The mixes with RS possess denser ITZ with fewer voids, whereas the ITZ in the mixes with IBA possess weaker ITZ with higher micro-cracks. Such higher micro-cracks in the ITZ results in the capillary suction of the free water available for the hydration. The IBA aggregates possess finer fractions that can either attribute to filler activity of pozzolanic reactivity [15, 16, 23]. The former mechanism results in the densification of micro-structure through direct filling whereas the latter densifies the micro-structure with the formation of supplementary C–S–H. Joseph *et al.* [53] and Tang *et al.* [55] inferred that well-graded IBA with prolonged curing show equivalent absorption with partial substitution of IBA. For instance, at 90 days, the water absorption of IBA30, IBA60, IBA90 and IBA 100 was only 5.50%, 12.77%, 21.95% and 25.19% higher than IBA0. The prolonged curing lowers the pore volume through the formation of hydration compounds that reduces the absorption in the concrete.

3.8. Microstructural investigations

Figure 12 shows the microstructure of the concrete mixes. Figure 12(a) shows the SEM image of IBA0 mix. The microstructure of IBA0 discloses a dense microstructure with CH crystals, ettringite (AFt) phases, and C–S–H gel. The incidence of C–S–H, a prime hydration compound, provides a comprehensible matrix that contributes to the enhanced concrete properties as observed in the control mixes. The compact packing of hydration compounds confines the pore connectivity, subsequent in higher strength and elastic modulus and lower water absorption. Such attribute correlates with the findings of Neville [56], that signified the effect of C–S–H in enhancing strength and stiffness.

Figure 12(b) shows the SEM image of IBA30 mix. The microstructure reflects higher pore connectivity than IBA0, yet still possess substantial quantities of C–S–H. The porous texture of IBA results in the formation of stress localized weak regions; nevertheless, the heterogeneous surface in the IBA supports the nucleation

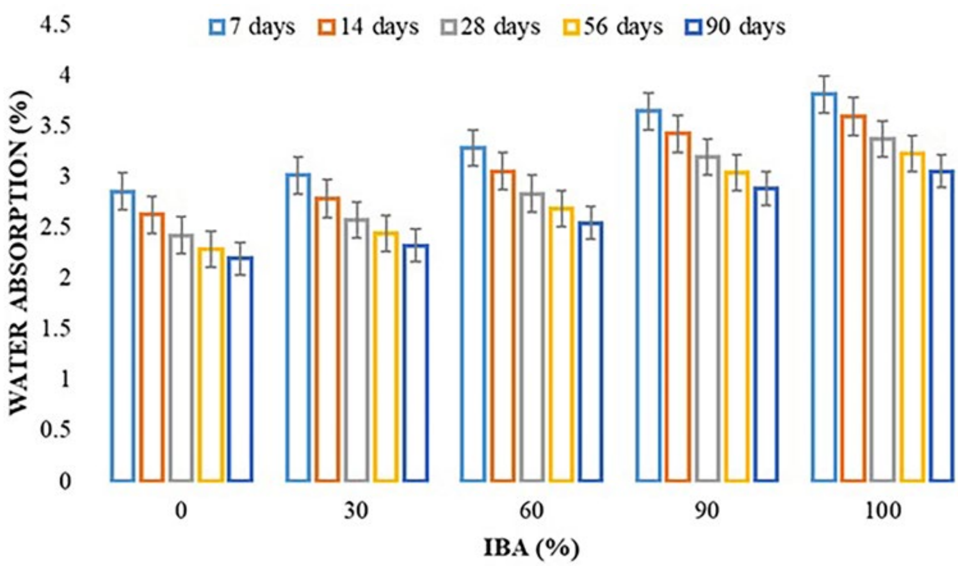

Figure 11: Water absorption.

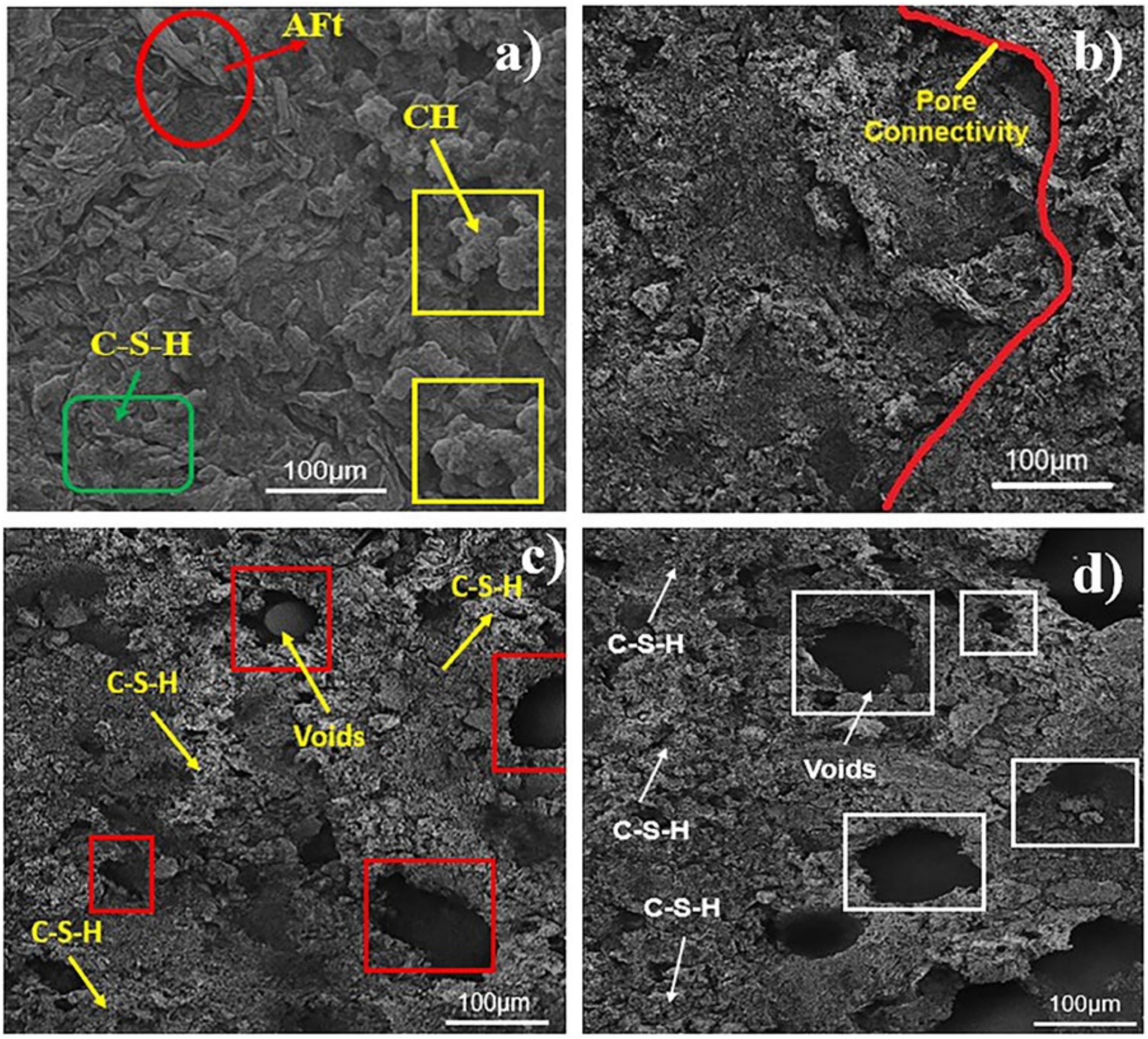

Figure 12: Microstructure of concrete mixes (a) IBA0, (b) IBA30, (c) IBA60, (d) IBA100.

of supplementary C–S–H, moderately overcoming for the density loss. Such attribute ensues in the modest decrease in the strength (7–13%) and an apparent reduction in the elastic modulus. The higher pore connectivity aligns with the higher porosity of IBA, as in [53], that reported the use of IBA augments capillarity owing to the matrix with partial densification of matrix.

Figure 12(c) shows the SEM image of IBA60 mix. The microstructure shows significant pores and huge pore-channels, disrupting the continuity C–S–H. The microstructure with unreacted/partially reacted and discontinues C-S-H network was evident. Such attribute directly reflects in the significant decreases in concrete properties showing up to 25–35% reduction, as the pores exhibit stress concentration. Similar observations are in the Figure 12(d) that show the SEM image of IBA100 mix. More discontinuous C–S–H gel with higher pore volume was evident in the microstructure that increases the stress concentration near the pores and thus inferior concrete properties were observed at higher substitution.

3.9. Correlation analysis

Figure 13 shows the correlation between various concrete properties. Linear relationship was established between various concrete properties owing the variation in the substitution percentage. It was also observed that the water absorption varies inversely with the strength, as the mix with lower absorption tend to show higher strength. The linear relationship among the variables varies from 0.9 to 1 showing higher correlation with maximum dependance among variables. The higher correlation results from the monotonic change in the replacement levels of IBA.

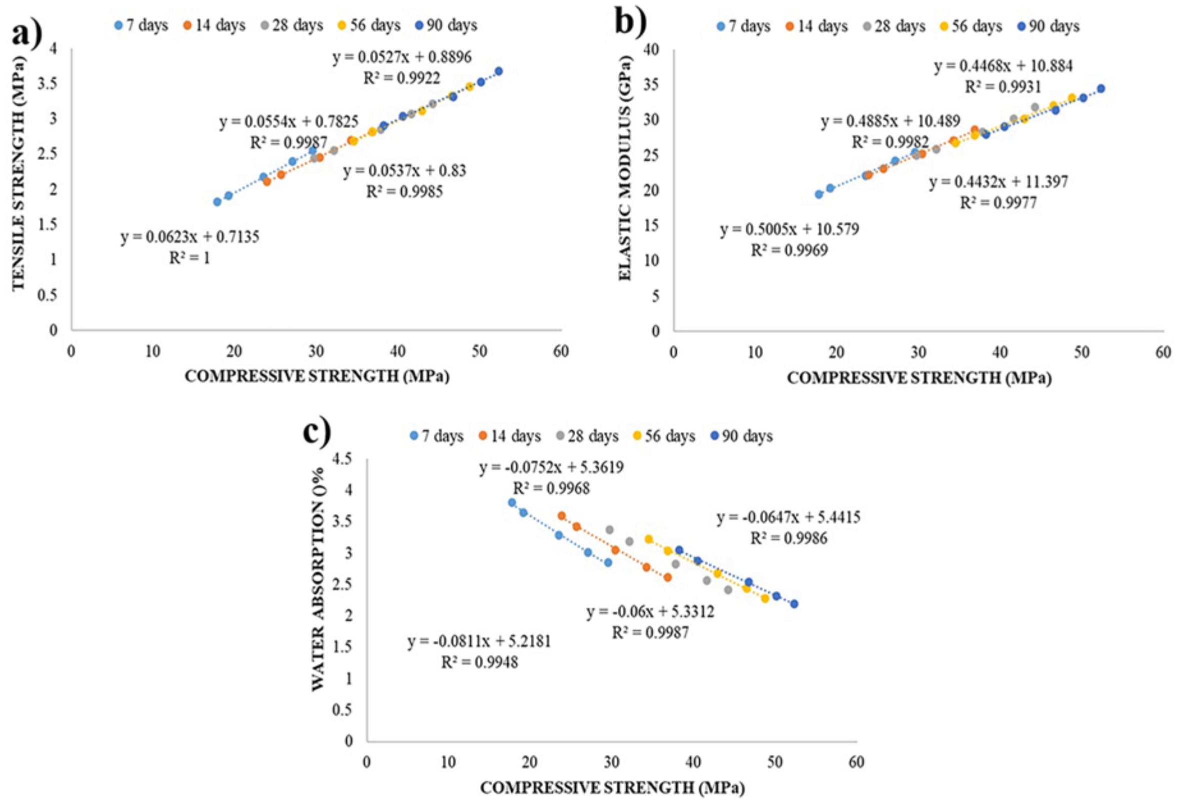

Figure 13: Correlation (a) compressive strength vs tensile strength, (b) compressive strength vs elastic modulus, (c) compressive strength vs water absorption.

4. DISCUSSIONS

The properties of concrete with IBA reflects a balance between two characteristics that IBA particles in a cementitious matrix include are dilution effect owing to highly porous, heterogenous and angular texture and a dormant filler/reactive component once fines, amorphous alumina/silica and carbonate phases involve in sealing the voids in the concrete. Mechanically, the inferior mechanical performance was observed for IBA mixes owing to weak ITZ and pore connectivity. The porous texture of IBA develops localization of stresses and more interconnected pores; upon loading these stress zones develop micro-cracks and decrease the stiffness and bridging ability [48, 57, 58]. Perhaps, the IBA possess substantial quantities of fine amorphous Al/Si phases with slow pozzolanic reactivity and filler attribute that densifies the pores and augments the micro-cracks around ITZ [51, 52]. Thus, IBA is neither "inert" nor consistently "reactive" material, yet the net effect relies on particle packing, presence of metals, mineralogy etc. Two practical significances were observed from the above mechanical property studies. Initially, literatures do not report single universal performance outcome of IBA in the concrete (at lower substitution) to important deteriorations (at higher replacement or without adequate pre-treatment). Secondly, curing period as prolonged curing exhibit partial strength recovery owing to deliberate pozzolanic reactivity that densifies the concrete matrix.

At lower substitution, the IBA acts as filler that seals the voids and forms hydration compounds resulting in improved concrete properties under prolonged curing. Several studies [52, 57] infer that optimized utilization of IBA found to improve the concrete properties and found to be environmentally friendly. As the percentage substitution increases, RS fractions dilute owing to the utilization of IBA with higher voids/pores. The hardened properties and transport properties shows negative effect upon its utilization and studies [20, 25, 31, 59] suggest suitable pre-treatments, effective particle packing and use of admixtures as measures to enhance the concrete properties. However, at complete substitution, collective effects such as pore connectivity, weaker ITZ, lower elastic modulus etc. results in deprived hardened properties, durability properties and undesirable structural behaviour for its intended structural applications [48, 50, 55]. Perhaps, certain applications even at higher substitution include non-load bearing walls, insulating members, geopolymer mixes, road layers etc. can support the possible utilization of IBA, though certain processing by washing/metal leaching/thermal treatment is required to improve the durability [53, 54, 57]. It was well observed that researches emphasize the pre-treatment of IBA. For instance, pre-washing lowers the salts and leaching of heavy metals, sieving eliminates large angular particles, thermal treatment reduces the LOI that improves the reactive phases and mechanical treatment through grinding improves the surface through grinding [11, 15, 53, 57, 59].

The excessive substitution of raw IBA tend to affect the concrete properties, and so studies suggest treatment of IBA before its utilization. Several studies [14, 15, 20] emphasize different dimensions of influence of curing regime on the properties of IBA concrete. The prolonged curing counteracts the negative dilution effect owing to the higher porosity of IBA with the positive secondary hydration effect with the formation of supplementary C–S–H and filler attribute. The prolonged curing increases the water availability for the formation of hydration compounds and dissolution of Si/Al in IBA, which then support in the formation of supplementary C–S–H. Such attribute refines the pores structure and improves the ITZ. The findings of the study also show reduction in the strength loss with increase in the curing period. Nevertheless, curing does not completely eradicate the negative effects of IBA. The IBA comprises of minerals such as feldspar, silica and calcite with amorphous phase. The latter amorphous phases interact slowly, and the crystalline phases tend to remain inert and lowering the stiffness and mechanical properties. Furthermore, even small proportions of metal scraps and aluminum in IBA reacts under alkaline environment to produce hydrogen, resulting in concrete expansion that necessitates the treatments before its utilization. The engineering perspective should consider curing as integral design part in IBA mixes for enhanced properties. The extensive research and literature discussions from past researches emphasize that IBA should be treated to evaluate the LOI, mineralogy with effective particle packing before its use. Furthermore, to enhance the latent reactivity, it is recommended to pre-treat the IBA with prolonged curing as design strategy to improve the concrete properties. For their intended structural applications, it is recommended to restrict the percentage utilization or utilize it in the non-structural applications. The afore-mentioned outcomes of the research promote the effective utilization of dumped IBA overcoming the landfill degradation and promote sustainability in the construction.

5. CONCLUSIONS

The research investigates the utilization of treated incinerated bottom ash (IBA) as a substitute to fine aggregate in the concrete, with proportions varying from 0% to 100% and assessed at various curing periods. The research aim was to investigate the effect of IBA on the fresh, hardened and microstructural characteristics of concrete, supported with correlation analysis. Based on the experimentation, the following conclusions are drawn as follows:

1. The properties of IBA are inferior than RS exhibiting lower specific gravity and higher absorption. The chemical composition of IBA reveal amorphous phases that delays the pozzolanic reaction and the morphology reflects the angular and porous texture compared to rounded and non-porous texture of RS.
2. The workability of concrete lowers with the substitution of IBA showing a maximum of 17.39% with 100% IBA. The angular and porous IBA captivates more mixing water, lowering the flowability of the mixes.
3. The maximum reduction of 33%, 23.98%, 26.62% and 21.38% was observed for compression, tension, flexure and elastic modulus properties of concrete with 100% of IBA. The higher porosity of IBA and the consequent weak ITZ attributes to the inferior hardened properties in the concrete.
4. The water absorption increases with the substitution of IBA showing an augmentation from 5.78% to 28.14% owing to the pore-connectivity ensuing from the porous texture of IBA.
5. Prolonged curing of IBA concrete tend to pronounce better results in strength gain than RS concrete. The delayed reactivity of IBA in the formation of supplementary C–S–H reduces the strength loss in the concrete.
6. Microstructure reveal the incidence of hydration compounds and ettringite with fewer pores in RS concrete, while the IBA concrete reflects the incidence of discontinuous C–S–H with pore volume. The volume of pores and C–S–H discontinuity augments with the higher substitutions of IBA.

The research recommends the optimal utilization of treated IBA and prolonged curing improves its structural applications, while higher substitution can intend its non-structural applications such as non-load bearing walls, paver blocks, road layers etc.

6. BIBLIOGRAPHY

[1] WORLD BANK, *What a waste 2.0*, https://datatopics.worldbank.org/what-a-waste, accessed in January, 2026.

[2] ENVIRONMENTAL PROTECTION AGENCY USA, *Environmental statistics and data*, https://www.epa.gov, accessed in January, 2026.

[3] DEPARTMENT OF ENVIRONMENT FOOD & RURAL AFFAIRS, *UK statistics on waste*, https://www.gov.uk/government/statistics/uk-waste-data, accessed in January, 2026.

[4] MINISTRY OF ENVIRONMENT JAPAN, *Municipal solid waste generation and disposal*, https://www.env.go.jp/en/press/press_01276.html, accessed in January, 2026.

[5] REN, Z., ZUO, G., "Challenges of implementing municipal solid waste separation policy in China", *Sustainability*, v. 16, n. 18, pp. 8081, 2024. doi: https://doi.org/10.3390/su16188081.

[6] CENTRAL POLLUTION CONTROL BOARD*, Annual report 2020–21 on implementation of solid waste management rules*, New Delhi, CPCB, 2016.

[7] INTERGOVERNMENTAL PANEL ON CLIMATE CHANGE, *Climate change 2021: the physical science basis – Contribution of Working Group I to the Sixth Assessment Report of the Intergovernmental Panel on Climate Change*, Cambridge, Cambridge University Press, 2021.

[8] ASTRUP, T.F., TONINI, D., TURCONI, R., *et al.*, "Life cycle assessment of thermal waste-to-energy technologies: Review and recommendations", *Waste Management*, v. 37, pp. 104–115, 2015. doi: https://doi.org/10.1016/j.wasman.2014.06.011. PubMed PMID: 25052337.

[9] KLEIB, J., AOUAD, G., ABRIAK, N.E., *et al.*, "Production of Portland cement clinker from French municipal solid waste incineration bottom ash", *Case Studies in Construction Materials*, v. 15, pp. e00629, 2021. doi: https://doi.org/10.1016/j.cscm.2021.e00629.

[10] TANG, P., CHEN, W., XUAN, D.X., *et al.*, "Investigation of cementitious properties of different constituents in municipal solid waste incineration bottom ash as supplementary cementitious materials", *Journal of Cleaner Production*, v. 258, pp. 120675, 2020. doi: https://doi.org/10.1016/j.jclepro.2020.120675.

[11] ABRIL, A.J., SAVAL, J.M., CUENCA, A., "Using sewage-sludge ash as filler in bituminous mixes", *Journal of Materials in Civil Engineering*, v. 27, pp. 401–414, 2015.

[12] ZHU, Y., ZHAO, Y., ZHAO, C., *et al.*, "Physicochemical characterization and heavy metals leaching potential of municipal solid waste incinerated bottom ash (MSWI-BA) when utilized in road construction", *Environmental Science and Pollution Research International*, v. 27, n. 12, pp. 14184–14197, 2020. doi: https://doi.org/10.1007/s11356-020-08007-9. PubMed PMID: 32040740.

[13] LIU, J., FAN, X., LI, Z.L., *et al.*, "Novel recycling application of high volume municipal solid waste incineration bottom ash (MSWIBA) into sustainable concrete", *The Science of the Total Environment*, v. 838, n. Pt 2, pp. 156124, 2022. doi: https://doi.org/10.1016/j.scitotenv.2022.156124. PubMed PMID: 35605859.

[14] SHEN, P.L., ZHENG, H.B., XUAN, D.X., *et al.*, "Feasible use of municipal solid waste incineration bottom ash in ultra-high-performance concrete", *Cement and Concrete Composites*, v. 114, pp. 103814, 2020. doi: https://doi.org/10.1016/j.cemconcomp.2020.103814.

[15] HOLMES, N., O'MALLEY, H., CRIBBIN, P., *et al.*, "Performance of masonry blocks containing different proportions of incinerator bottom ash", *Sustainable Materials Technologies*, v. 8, pp. 14–19, 2016. doi: https://doi.org/10.1016/j.susmat.2016.05.001.

[16] LI, X.G., LIU, Z.L., LV, Y., *et al.*, "Utilization of municipal solid waste incineration bottom ash in autoclaved aerated concrete", *Construction & Building Materials*, v. 178, pp. 175–182, 2018. doi: https://doi.org/10.1016/j.conbuildmat.2018.05.147.

[17] XIE, R., XU, Y., HUANG, M., *et al.*, "Assessment of municipal solid waste incineration bottom ash as a potential road material", *Road Materials and Pavement Design*, v. 18, n. 4, pp. 992–998, 2017. doi: https://doi.org/10.1080/14680629.2016.1206483.

[18] SUN, Y.U., JI, L., LIAO, J., *et al.*, "Performance analysis and prediction of asphalt pavement containing municipal solid waste incineration bottom ash aggregate based on MEPDG", *Scientific Reports*, v. 15, n. 1, pp. 7597, 2025. doi: https://doi.org/10.1038/s41598-025-91686-6. PubMed PMID: 40038381.

[19] OLEA, P.E.S., BURKE, I.T., MOHAMMAD, A., *et al.*, "Reuse potential of municipal solid waste incinerator bottom ash as secondary aggregate: Material characteristics, persistent organic pollutant content and effects of pH and selected environmental lixiviants on leaching behaviour", *Waste Management*, v. 187, pp. 262–274, 2024. doi: https://doi.org/10.1016/j.wasman.2024.07.026. PubMed PMID: 39079254.

[20] FAN, X.U., LI, Z., ZHANG, W., *et al.*, "Effects of different supplementary cementitious materials on the performance and environment of eco-friendly mortar prepared from waste incineration bottom ash", *Construction & Building Materials*, v. 356, pp. 129277, 2022. doi: https://doi.org/10.1016/j.conbuildmat.2022.129277.

[21] YAO, J., SONG, H., LI, Y., *et al.*, "Mechanism of macro- and microscopic performance of cement mortars influenced by municipal solid waste incineration bottom ash as sand substitution", *Construction & Building Materials*, v. 397, pp. 132317, 2023. doi: https://doi.org/10.1016/j.conbuildmat.2023.132317.

[22] HUYNH, T.P., NGO, S.H., "Waste incineration bottom ash as a fine aggregate in mortar: An assessment of engineering properties, durability, and microstructure", *Journal of Building Engineering*, v. 52, pp. 104446, 2022. doi: https://doi.org/10.1016/j.jobe.2022.104446.

[23] ALDERETE, N.M., JOSEPH, A.M., VAN DEN HEEDE, P.V.D., *et al.*, "Effective and sustainable use of municipal solid waste incineration bottom ash in concrete regarding strength and durability", *Resources, Conservation and Recycling*, v. 167, pp. 105356, 2021. doi: https://doi.org/10.1016/j.resconrec.2020.105356.

[24] LIU, J., REN, Y., CHENG, L., *et al.*, "Unlocking the potential of municipal solid waste incineration bottom ash into sustainable fine aggregates for production of eco-friendly lightweight sprayed mortar", *Journal of Building Engineering*, v. 108, pp. 112880, 2025. doi: https://doi.org/10.1016/j.jobe.2025.112880.

[25] JOSEPH, A.M., SNELLINGS, R., NIELSEN, P., *et al.*, "Pre-treatment and utilisation of municipal solid waste incineration bottom ashes towards a circular economy", *Construction & Building Materials*, v. 260, pp. 120485, 2020. doi: https://doi.org/10.1016/j.conbuildmat.2020.120485.

[26] REN, P., MEHDIZADEH, H., LING, T.C., "Performance investigation of the artificial aggregate by integrally recycling incineration bottom ash and fly ash", *Cement and Concrete Composites*, v. 152, pp. 105678, 2024. doi: https://doi.org/10.1016/j.cemconcomp.2024.105678.

[27] CHIMENOS, J.M., CUSPOCA, F., MALDONADO-ALAMEDA, A., *et al.*, "MSW incineration bottom ash-based alkali-activated binders as an eco-efficient alternative for urban furniture and paving: Closing the loop towards sustainable construction solutions", *Buildings (Basel, Switzerland)*, v. 15, n. 9, pp. 1571, 2025. doi: https://doi.org/10.3390/buildings15091571.

[28] WANG, C., ZHAO, X.I., ZHANG, X.I., *et al.*, "Study of waste incineration bottom ash as fine aggregate applied to green alkali-activated bottom ash-slag concrete: Mechanical properties, microstructure, durability", *Construction & Building Materials*, v. 449, pp. 138484, 2024. doi: https://doi.org/10.1016/j.conbuildmat.2024.138484.

[29] WANG, Q., CHU, H., LI, F., "Incorporating incineration bottom ash in environmentally friendly ultra- high-performance concrete: Impact on mechanical properties, durability, and environmental benefits", *Construction & Building Materials*, v. 481, pp. 141640, 2025. doi: https://doi.org/10.1016/j.conbuildmat. 2025.141640.

[30] BAYUSENO, A.P., SCHMAHL, W.W., "Understanding the chemical and mineralogical properties of municipal solid waste incineration (MSWI) bottom ash", *Waste Management*, v. 30, pp. 1509–1520, 2010. doi: https://doi.org/10.1016/j.wasman.2010.03.010. PubMed PMID: 20381330.

[31] LIN, K.L., WANG, K.S., TZENG, B.Y., *et al.*, "Effect of aging treatment on the engineering properties of MSWI bottom ash", *Journal of Hazardous Materials*, v. 163, pp. 600–606, 2018.

[32] TANG, P., FLOREA, M.V.A., SPIESZ, P., *et al.*, "Characteristics and application potential of municipal solid waste incineration (MSWI) bottom ashes: A review", *Construction & Building Materials*, v. 236, pp. 117578, 2021.

[33] WEI, Y., POON, C.S., WONG, Y.L., "Optimizing the use of municipal solid waste incineration bottom ash in cement-based materials", *Cement and Concrete Composites*, v. 114, pp. 103779, 2020.

[34] AMERICAN SOCIETY FOR TESTING AND MATERIALS, *ASTM C150/C150M-24 Standard specification for Portland Cement*, West Conshohocken, ASTM, 2018.

[35] AMERICAN SOCIETY FOR TESTING AND MATERIALS, *ASTM C33/C33M Standard specification for aggregates*, West Conshohocken, ASTM, 2018.

[36] BUREAU OF INDIAN STANDARDS, *IS 456 Plain and reinforced concrete – code of practice*, Bureau of Indian Standards, New Delhi, 2009.

[37] BUREAU OF INDIAN STANDARDS, *IS 10262 Guidelines for concrete mix design proportioning*, Bureau of Indian Standards, New Delhi, 2019.

[38] BUREAU OF INDIAN STANDARDS, *IS 5515 Specification compacting factor apparatus*, Bureau of Indian Standards, New Delhi, 1983.

[39] AMERICAN SOCIETY FOR TESTING AND MATERIALS, *ASTM C39/C39M-23 Standard test method for compressive strength of cylindrical concrete specimens*, West Conshohocken, ASTM, 2018.

[40] AMERICAN SOCIETY FOR TESTING AND MATERIALS, *ASTM C78/C78M-22 Standard test method for flexural strength of concrete (using simple beam with third-point loading)*, West Conshohocken, ASTM, 2018.

[41] AMERICAN SOCIETY FOR TESTING AND MATERIALS, *ASTM C469/C469M-22 Standard test method for static modulus of elasticity and Poisson's ratio of concrete in compression*, West Conshohocken, ASTM, 2018.

[42] AMERICAN SOCIETY FOR TESTING AND MATERIALS, *ASTM C642-21 Standard test method for density, absorption, and voids in hardened concrete*, West Conshohocken, ASTM, 2018.

[43] FORTEZA, R., FAR, M., SEGUI, C., *et al.*, "Characterization of bottom ash in municipal solid waste incinerators for its use in road base", *Waste Management*, v. 24, n. 9, pp. 899–909, 2004. doi: https://doi.org/10.1016/j.wasman.2004.07.004. PubMed PMID: 15504667.

[44] SIDDIQUE, R., " Utilization of municipal solid waste (MSW) ash in cement and mortar", *Resources, Conservation and Recycling*, v. 54, n. 12, pp. 1037–1047, 2010. doi: https://doi.org/10.1016/j.resconrec.2010.05.002.

[45] WANG, C., ZHAO, X.I., ZHANG, X.I., *et al.*, "Study of waste incineration bottom ash as fine aggregate applied to green alkali-activated bottom ash-slag concrete: Mechanical properties, microstructure, durability", *Construction & Building Materials*, v. 449, pp. 138484, 2024. doi: https://doi.org/10.1016/j.conbuildmat.2024.138484.

[46] CHIMENOS, J.M., CUSPOCA, F., MALDONADO-ALAMEDA, A., *et al.*, "MSW incineration bottom ash-based alkali-activated binders as an eco-efficient alternative for urban furniture and paving: Closing the loop towards sustainable construction solutions", *Buildings (Basel, Switzerland)*, v. 15, n. 9, pp. 1571, 2025. doi: https://doi.org/10.3390/buildings15091571.

[47] OLEA, P.E.S., BURKE, I.T., MOHAMMAD, A., *et al.*, "Reuse potential of municipal solid waste incinerator bottom ash as secondary aggregate: Material characteristics, persistent organic pollutant content and effects of pH and selected environmental lixiviants on leaching behaviour", *Waste Management*, v. 187, pp. 262–274, 2024. doi: https://doi.org/10.1016/j.wasman.2024.07.026. PubMed PMID: 39079254.

[48] CHO, B.H., NAM, B.H., AN, J., *et al.*, "Municipal solid waste incineration (MSWI) ashes as construction materials—a review", *Materials*, v. 13, n. 14, pp. 3143, 2020. doi: https://doi.org/10.3390/ma13143143. PubMed PMID: 32679661.

[49] FLOREA, M.V.A., BROUWERS, H.J.H., "Characteristics and application potential of MSWI bottom ashes: a review", *Construction & Building Materials*, v. 236, pp. 117578, 2019.

[50] TANG, P., FLOREA, M.V.A., SPIESZ, P., *et al.*, "Characteristics and application potential of MSWI bottom ashes: a review", *Construction & Building Materials*, v. 236, pp. 117578, 2021.

[51] BAYUSENO, A.P., SCHMAHL, W.W., "Understanding the chemical and mineralogical properties of the inorganic portion of MSWI bottom ash", *Waste Management*, v. 30, pp. 1509–1520, 2010. doi: https://doi.org/10.1016/j.wasman.2010.03.010. PubMed PMID: 20381330.

[52] CHEN, B., YE, G., "The role of water-treated municipal solid waste incineration (MSWI) bottom ash in microstructure formation and strength development of blended cement pastes", *Cement and Concrete Research*, v. 178, pp. 107440, 2024. doi: https://doi.org/10.1016/j.cemconres.2024.107440.

[53] JOSEPH, A.M., SNELLINGS, R., VAN DEN HEEDE, P.V., *et al.*, "The use of municipal solid waste incineration ash in various building materials: a Belgian point of view", *Materials*, v. 11, n. 1, pp. 141, 2018. doi: https://doi.org/10.3390/ma11010141. PubMed PMID: 29337887.

[54] ZHANG, T., ZHAO, Y., GAO, J., "Potential utilization of municipal solid waste incineration bottom ash in construction: A review", *Waste Management*, v. 60, pp. 267–279, 2016.

[55] TANG, P., FLOREA, M.V.A., BROUWERS, H.J.H., "Characterization of MSWI bottom ash for potential use in building materials", *Resources, Conservation and Recycling*, v. 102, pp. 54–65, 2015.

[56] NEVILLE, A.M., *Properties of concrete*, 5 ed., London, Pearson, 2011.

[57] LYNN, C., DHIR, R., GHATAORA, G., "Municipal incinerated bottom ash characteristics and potential for use as aggregate in concrete", *Construction & Building Materials*, v. 127, pp. 504–517, 2016. doi: https://doi.org/10.1016/j.conbuildmat.2016.09.132.

[58] SHANMUGAM, R., SELVAPRIYA, R., JAMUNA, M., *et al.*, "A study on high calcium flyash blended geopolymer composite with industrial derivatives", *Matéria*, v. 29, n. 4, pp. e20240646, 2024. doi: https://doi.org/10.1590/1517-7076-rmat-2024-0646.

[59] PACHECO, F., MOREIRA, M.A.B., KUWAKOWISKI, M.P., *et al.*, "Coal bottom ash characterization aiming the incorporation in cellular concrete", *Matéria*, v. 26, n. 3, pp. e13007, 2021. doi: https://doi.org/10.1590/s1517-707620210003.13007.